academicJournals

Vol. 10(2), pp. 15-27, February, 2018
DOI: 10.5897/JGMR2017.0284
Article Number: 792EFD856372
ISSN 2006-9766
Copyright © 2018
Author(s) retain the copyright of this article
http://www.academicjournals.org/JGMR

Journal of Geology and Mining Research

*Full Length Research Paper*

# Study of the roof behavior in longwall gob in long-term condition

**Mohammad Rezaei[1*], Abbas Majdi[2], Mohammad Farouq Hossaini[2] and Iraj Najmoddini[1]**

[1]Department of Mining Engineering, Faculty of Engineering, University of Kurdistan, Sanandaj, Iran.
[2]School of Mining Engineering, College of Engineering, University of Tehran, Tehran, Iran.

Received 18 November, 2017; Accepted 4 January, 2018

**Assessment of the roof behavior in longwall gob and estimation of the occurrence of caving and fracturing zones above mined panels are the main factors used in evaluating abutment stresses, ground subsidence, face support and adjacent structures design. The combined height of caving and fracturing zones is taken as equivalent to the height of destressed zone (HDZ) in this study. The long-term estimation of this height plays a key role in accurate determination of maximum ground surface subsidence and the amount of transferred loads towards the neighboring solid sections. In this paper, the roof behavior in longwall gob has been studied in long-term condition. For this purpose, a time-dependent model based on the energy balance in longwall mining combined with a rheological model of caved materials with time-varying parameters was used to calculate HDZ. Also, parametric study was conducted to evaluate the effects of geometrical and geomechanical parameters on the roof caving and fracturing. Moreover, the calculated HDZ from the current study is compared with the results of the existing numerical, analytical and empirical models and the *in-situ* measurements reported in literatures. Comparative study confirms a good agreement that exists between the results of the present study with those of the *in-situ* measurements and empirical models. It can be concluded that the results of this research can be successfully used to evaluate HDZ in longwall gob in long-term condition to determine the induced stress and surface subsidence in longwall mining.**

**Key words:** Longwall mining, height of destressed zone, time-dependent model, strain energy, rheological model.

## INTRODUCTION

Longwall mining method is the most popular and high production method used for coal extraction in the world. This method is suitable for the extraction of relatively thick, slightly horizontal and uniform coal seams. The overall objective of coal mining is to obtain maximum productivity with reliable safety considerations. Besides that, mining efficiency exclusively depends on the stability of the gates, tunnels, pillars and stopes. The stability of these structures is also related to both the roof cave-in performance and the interaction of the caved materials with the roof rock strata. After extracting the coal seam and advancing the hydraulic jacks, the immediate roof of

*Corresponding author. E-mail: m.rezaei@uok.ac.ir. Tel: +988733660073. Fax: +988733668513.

Author(s) agree that this article remain permanently open access under the terms of the Creative Commons Attribution License 4.0 International License

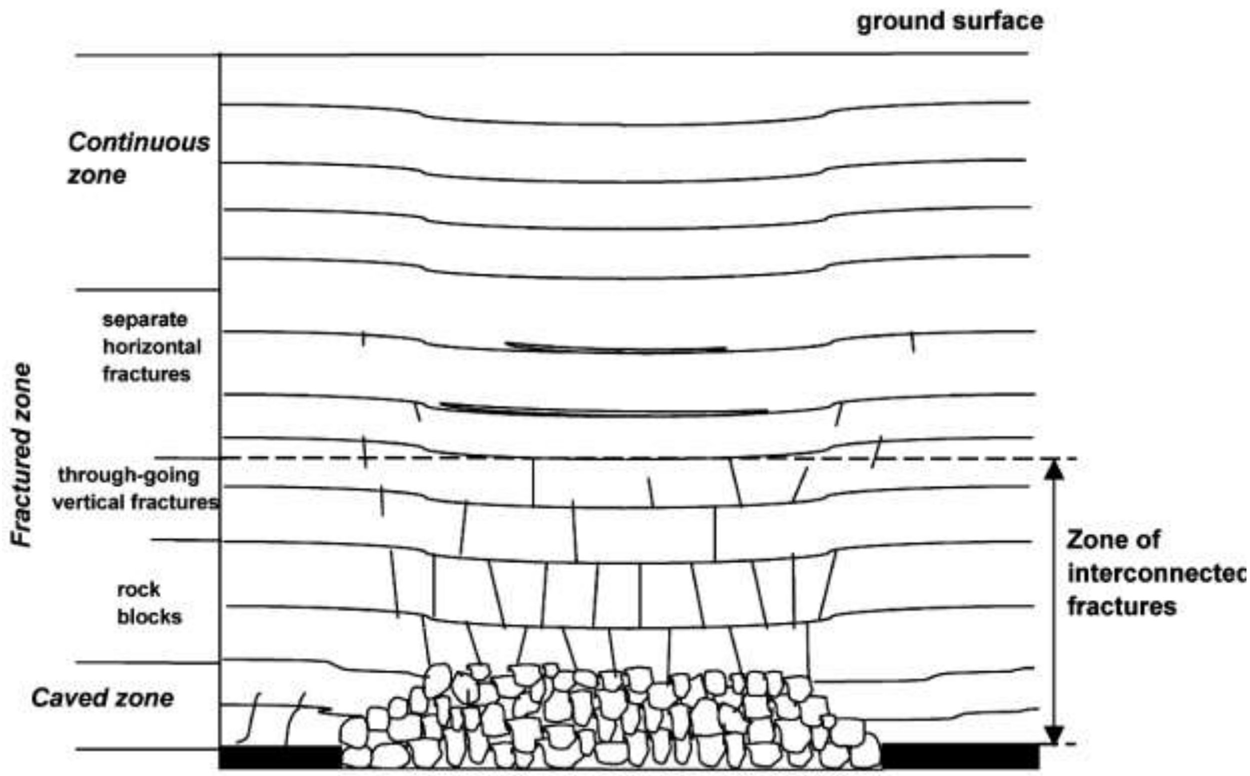


**Figure 1.** Disturbed zones due to excavation of a panel in longwall mining.
Source: Palchik (2003).

the mined area collapses and caves into the void area behind the working face. The downward movement of the roof strata then gradually extends upwards and will cause the disturbed roof strata to become destressed. Thus, the overburden pressure above the destressed zone will be redistributed in the rock mass surrounding longwall panels directed to the front abutment and the two adjacent neighboring solid sections (Majdi and Rezaei, 2013; Rezaei et al., 2015a, 2015b, 2017; Rezaei, 2016, 2017).

There are common approaches for analyzing the fracturing and caving behavior of the panel roof rock strata including *in-situ* measurement and physical, empirical, numerical and analytical modeling. Although the *in-situ* tests and physical modeling provide useful and reliable results, they are time consuming and expensive (Rezaei et al., 2015a). On the other hand, empirical methods are based on the data extracted from a specific case study with particular characteristics and are not qualified for other cases with different mechanical or physical properties. Numerical modeling is widely used in this field particularly as a tool for assessing the caving progress. However, this method is time consuming and requires a large number of input variables which depend on the available data; this may need to be estimated or assumed. Thus several researchers have proposed mathematical methods to study the roof behavior over the mined panel in longwall mining.

Many researchers have investigated the behavior of roof rock strata, process of the gradual upward movement and determination of the height of caving and fracturing zones (Rezaei et al., 2017). According to these studies, it is concluded that there are zones of disturbance above the mined panel (Figure 1). These zones include caved, fractured and continuous deformation zones (Palchik, 2003). The extent of each zone depends on the geological and geomechanical properties of overburden strata including the strength characteristics of rocks, the *in-situ* stress, the thickness of coal seam, and overburden stress and the type and nature of the strata (Gao et al., 2014).

In the field of the current research topic, Rezaei (2016) and Rezaei et al. (2017) studied the roof caving and fracturing using the traditional and multilayer perceptron (MLP) artificial neural networks (ANNs), respectively. According to these studies, traditional and multilayer perceptron ANN models predict the height of destressed zone 3.1-86.5 and 2.4-81.64 times the extracted coal seam thickness, respectively. Sheng et al. (2017) applied the combination of borehole photography and the seismic CT scanner techniques to determine the height of caved and fractured zones over the longwall panel in a case study. Liu et al. (2017) studied the height of the water-flowing fractured zone based on the *in-situ* measurement,

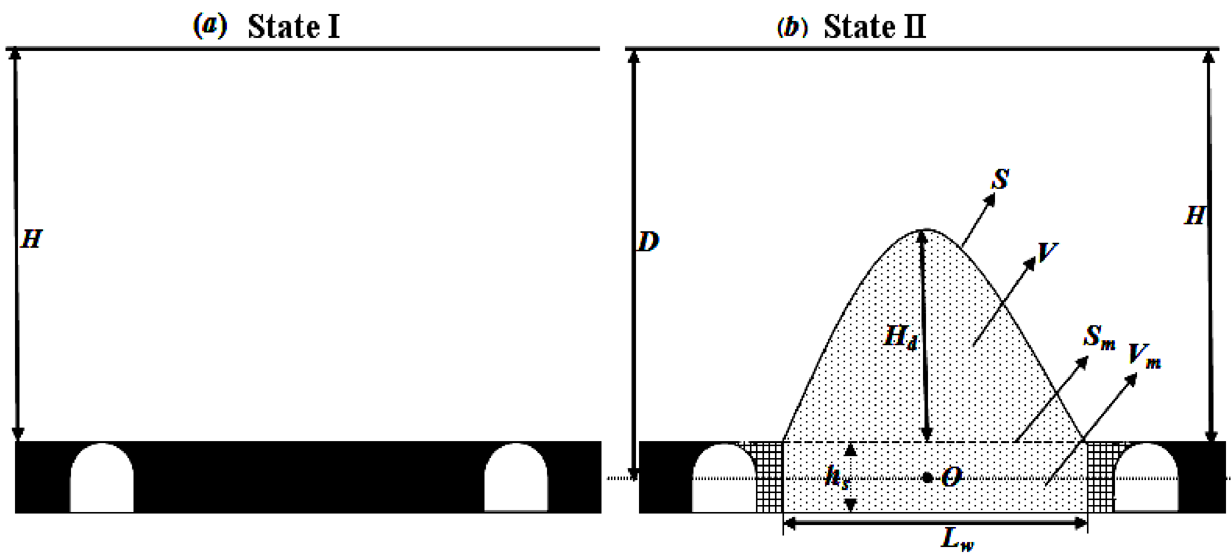


**Figure 2.** Longwall mining configuration: (*a*) before panel extraction or state I and (*b*) after complete extraction of a longwall panel or state II.
Source: Rezaei et al. (2015a).

mechanical theory calculation and numerical simulation. Wang et al. (2017) evaluated the separation and fracturing in the undermined overburden pressure using the theoretical and numerical models. They showed that theoretical model is suitable to quantify the extent of possible risk zones. Literature review in this field shows that there are many factors that can influence the roof strata behavior. These factors include coal seam characteristics, roof rock strata properties, stress conditions, etc (Le et al., 2017). However, all of these effective parameters were not simultaneously considered in the study of roof behavior in the previous investigations. An effort is made in the current study to overcome this limitation for improving the related results.

In order to study the roof behavior over the longwall panel in this study, the combination of the caving and fracturing zones is considered as the height of destressed zone (HDZ). Beyond this height, the induced stress due to the overburden depth will be transferred towards the adjacent solid sections. Therefore, height of destressed zone can play a vital role in the amount of transferrable stresses to front abutment, adjacent access tunnels, pillars and panel rib-sides. Accordingly, to suitably evaluate the amount of transferrable loads to the adjacent gates and the intervening pillars, the height of destressed zone must be estimated. The main objective of this paper is to study the roof behavior based on the determination of the HDZ over the longwall gob in long-term condition. The HDZ determination was conducted on the basis of the strain energy balance in longwall coal mining and a nonlinear rheological model of caved materials. In order to cover the available problems in previous researches, the effects of geometric parameters, roof rock strata strength properties, pressure time and temperature-dependent parameters of caved materials were considered in determining the height of destressed zone in this research.

## METHODOLOGY

In this research, an extension model of the proposed one by Rezaei et al. (2015b) is used to study the roof behavior over the longwall gob in long-term condition. For this, the basic concept of energy consideration in longwall mining along with the calculation of the energy component in this area is discussed in detail.

### Basic conceptual model

The concept of strain energy balance in longwall mining was firstly introduced and discussed by Rezaei et al. (2015a). In their opinion, longwall panel and its surrounding rock mass can be considered as a separate system in which the equilibrium between its energy components should be maintained. On this basis, as the extraction of coal seam from the panel starts in the longwall mining, the energy balance within the system enclosing the mine openings and surrounding rocks is distorted. However, energy balance must be preserved before and after the mining. A schematic configuration of longwall mining pre and post-mining is shown in Figure 2 in which states I and II are considered as the primary status and the end of coal (rock) extraction inside a panel, respectively (Rezaei et al., 2015a). In Figure 2, $L_w$ is the panel width, $H$ is the depth of cover, $h_s$ is the extracted seam thickness, $H_d$ is the height of destressed zone, $D$ is the distance of horizontal line across the centre of gravity of the panel to the ground surface, $V_m$ is the volume of mined panel, $S_m$ is the surface of mined panel, and $V$ and $S$ are the volume and surface of destressed zone above a panel.

By extracting the coal layers, the total stored strain energy in the mined rock (coal) is released and consumed in failing, caving and destressing the panel roof rock strata (Rezaei et al., 2015a). This process continues until the extraction of a longwall panel completed. At the end of panel extraction and after the total compression of caved materials, a defined zone with height of $H_d$ is normally formed above the mined panel which can be called "destressed zone" (Figure 2b). Therefore, it can be concluded that the stored strain energy in the mined rock (coal) should be equal to the stored strain energy in caved rocks within the destressed zone as given in Equation 1. Based on the stated equation, the height of destressed zone (HDZ) was analytically determined in short-term condition. The stored strain energy in the mined rock ($U_m$) is the same in long and short-terms conditions but the stored strain energy in the caved rocks within destressed zone ($U_d$) certainly is different.

$$U_m = U_d \tag{1}$$

where $U_m$ is the stored strain energy in the mined rock (coal) and $U_d$ is the stored strain energy in the caved rocks within the destressed zone.

**Determining the stored strain energy in the mined area**

For long-term calculation of the HDZ, the stored strain energy in the extracted coal (rock) seam ($U_m$) and the stored strain energy in the destressed zone ($U_d$) should be determined in long-term conditions. The HDZ can be obtained by equaling these two mentioned energy components. Due to the complex conditions of longwall mining, those general assumptions that considered by Rezaei et al. (2015a) in calculating the involved energy components are also regarded here. The difference between the long-term calculation of HDZ in this research with the time-independent energy model proposed by Rezaei et al. (2015a) is in the stored strain energy within the destressed zone ($U_d$). Calculation of this component is outlined in the following sub-section. However, the stored strain energy in the extracted coal (rock) seam before any extraction ($U_m$) is similar in short-term and long-term conditions because mining is not started yet in both states. Therefore, the equation developed by Rezaei et al. (2015a) is utilized here for $U_m$ calculation in this study:

$$U_m = \frac{(1+\nu)(1-2\nu)\gamma A_m \sigma_v}{2(1-\nu)E}\left[\frac{h_s^2}{3} + H^2 + Hh_s\right] \tag{2}$$

where $U_m$ is the stored strain energy in the extracted coal (rock) seam, $\sigma_v$ is the initial stress due to overburden pressure which is equal to $\gamma H$, $H$ is the depth of cover, $\gamma$ is the panel roof rock's average unit weight, $h_s$ is the extracted coal (rock) seam thickness, $A_m$ is the cross section of the mined panel which is equal to the panel width multiplied by the extracted coal seam (rock) thickness ($L_w \times h_s$), $\nu$ is the panel roof rock's average Poisson ratio and $E$ is the panel roof rock's average elastic modulus.

**Determining the stored strain energy in the destressed zone**

The stored strain energy of caved materials within the destressed zone ($U_d$) is generally composed of elastic ($U_E$) and viscoplastic strain energies ($U_V$).

$$U_d = U_E + U_V \tag{3}$$

Under pressure of the roof in long-term conditions, the mechanical properties of the caved materials can change, so that the elastic modulus and the coefficient of viscosity of caved materials also change over the time. Thus, the viscoplastic strain energy of the caved materials should be considered in calculations. In this research, the rheological properties of the caved materials are considered according to the nonlinear rheological constitutive model established by Zhang et al. (2011). To investigate the rheological properties of the caved materials in this model, elastic modulus $(E)$, coefficient of viscosity $(\eta)$ and threshold value of stress ($\sigma_s$) is considered based on the modified Bingham model (Figure 3). Unlike previous models about the deformation of a structure, the elastic modulus and the coefficient of viscosity are the functions of time.

According to Zhang et al. (2011), the nonlinear rheological constitutive model can be described as:

$$\begin{cases} \sigma = E_0 e^{-at}\varepsilon & \sigma \le \sigma_s \\ \sigma = \dfrac{\varepsilon}{K} - \lambda\varepsilon, & \sigma > \sigma_s \end{cases} \tag{4}$$

where $\sigma$ is the stress of caved materials, $\sigma_s$ is the threshold value of stress, $E_0$ is the initial elastic modulus, $a$ is the material constant, $t$ is the pressure time of caved materials, $\varepsilon$ is the strain of caved materials, $\lambda$ is the slope of materials hardening stage and $K$ is the coefficient that is calculated by (Zhang et al., 2011):

$$K = \frac{1}{E_0 e^{-at}} + \frac{t^\alpha}{\eta_0 C\alpha\sigma_s^\mu} \tag{5}$$

where $\eta_0$ is the initial coefficient of viscosity and; $C$, $\mu$ and $\alpha$ are material coefficients related to temperature. Replacing the $B = 1/\eta_0 C\alpha$ into Equation 5 leads to:

$$K = \frac{1}{E_0 e^{-at}} + \frac{Bt^\alpha}{\sigma_s^\mu} \tag{6}$$

In Equation 4, the deformed caved materials have the viscoplastic properties when $\sigma$ approaches $\sigma_s$. Therefore, the caved materials system has the elastic properties when $\sigma \le \sigma_s$ and the

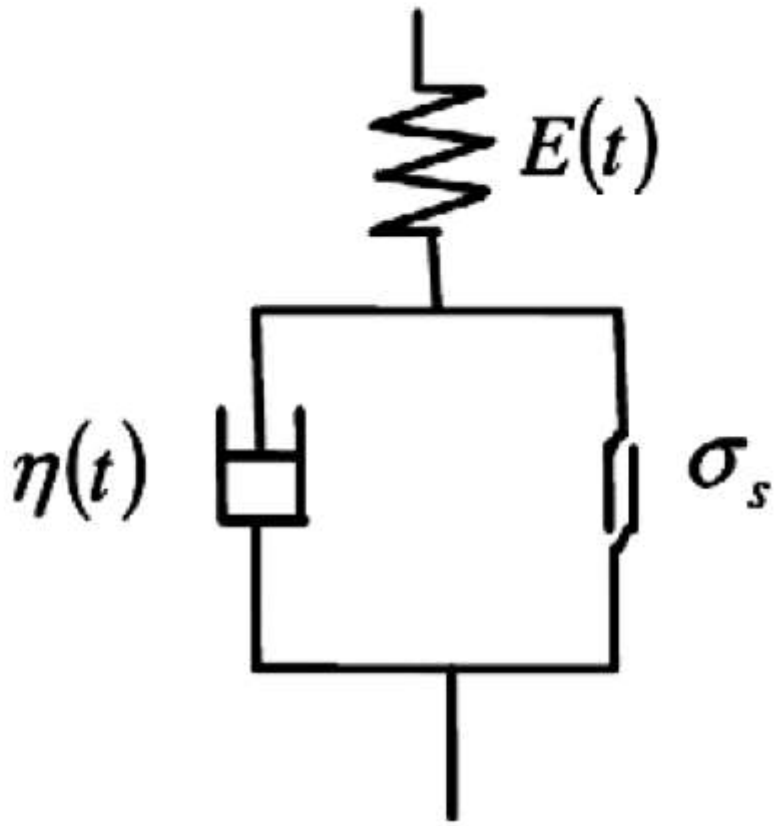


**Figure 3.** Modified Bingham model.
Source: Zhang et al. (2011).

viscoplastic properties when $\sigma > \sigma_s$. Accordingly, the elastic and viscoplastic components of strain energy can be calculated based on its associated stress.

To calculate the elastic strain energy of the caved materials within the destressed zone, the common equation of strain energy is used. If the destressed zone above the longwall panel is considered as a separate system (surface with height of $H_d$ in Figure 2b), its absorbed elastic strain energy can be calculated as follows:

$$U_E = \frac{1}{2}\int \sigma\varepsilon dV = \frac{1}{2}\int_0^h \sigma\varepsilon A dh \qquad (7)$$

where $\sigma$ is the applied stress on the caved materials, $\varepsilon$ is the strain occurring under the corresponding applied stress, $h$ is the height of the caved materials within the destressed zone and $A$ is the unit surface of the system. Here, $A_d$ is considered as the unit surface of destressed zone which is equal to the panel width multiplied by the unit length of longwall panel ( $A_d = L_w \times 1^m$ ). After the caving process is completed in which the caved materials are through compressed, no further caving will take place. This means that the caved materials are completely compacted and there is no void area for further roof caving. Therefore, the height of destressed zone will be constant and no increase. On this basis, released energy is consumed in the roof distressing with the height of $H_d$. Accordingly, it can be concluded that the total height of caved materials ($h$) can be equivalent to the height of destressed zone ($h = H_d$). By applying the aforementioned simplifications, Equation 7 is modified to:

$$U_E = \frac{1}{2}\sigma\varepsilon A_d H_d \qquad (8)$$

The substitution of the elastic part of Equation 4 into Equation 8 leads to:

$$U_E = \frac{1}{2}E_0 e^{-at} A_d H_d \varepsilon^2 \qquad (9)$$

In the aforementioned equation, $E_0$ is the initial elastic modulus which is taken as equivalent of elastic modulus ($E$) of the overburden rock mass. Thus, Equation 9 can be modified to:

$$U_E = \frac{1}{2}E e^{-at} A_d H_d \varepsilon^2 \qquad (10)$$

The following equation can be used to describe the stress-strain behaviour of caved materials (Salamon, 1990):

**Table 1.** Experimental parameters used in plotting of the graphs.

| $\sigma_s$ (MPa) | E (MPa) | B | μ | α | λ | a |
|---|---|---|---|---|---|---|
| 20 | 59 | 1.24 | 2 | 0.3 | 3 | 1 |

Source: Zhang et al. (2011).

$$\sigma_c = \frac{E_0 \varepsilon}{1 - \varepsilon / \varepsilon_m} \tag{11}$$

where $\sigma_c$ is the uniaxial compressive strength of caved materials, $\varepsilon$ is the strain occurring under the applied stress, $E_0$ is the initial elastic modulus which is considered same elastic modulus of rock mass ($E$) and $\varepsilon_m$ is the maximum possible strain of the bulked rock material.

From Equation 11, one can write:

$$\varepsilon = \frac{\sigma_c}{[E + \frac{\sigma_c}{\varepsilon_m}]} \tag{12}$$

The following equation is used to show the relationship between the maximum strain ($\varepsilon_m$) and the bulking factor ($b$) (Yavuz, 2004):

$$\varepsilon_m = \frac{b-1}{b} \tag{13}$$

Substituting Equation 13 for Equation 12 leads to:

$$\varepsilon = \frac{\sigma_c}{[E + \frac{b\sigma_c}{(b-1)}]} \tag{14}$$

Now by substitution of Equation 14 for Equation 9, the elastic stored strain energy in caved materials within the destressed zone ($U_d$) is calculated as follows:

$$U_E = \frac{E e^{-at} A_d H_d \sigma_c^2}{2[E + \frac{b\sigma_c}{(b-1)}]^2} \tag{15}$$

Similar method is applied to calculate the viscoplastic strain energy ($U_V$). The substitution of the viscoplastic part of Equation 4 for Equation 8 leads to:

$$U_V = (\frac{\varepsilon^2}{2K} - \frac{\lambda \varepsilon^2}{2}) A H_d \tag{16}$$

When Equation 14 substituted for Equation 16 and rearranged, the final equation of viscoplastic stored strain energy in caved materials within the destressed zone can be obtained:

$$U_V = \frac{A_d H_d \sigma_c^2}{2[E + \frac{b\sigma_c}{(b-1)}]^2}[\frac{1}{K} - \lambda] \tag{17}$$

Finally, the total stored strain energy in caved materials within the destressed zone ($U_d$) can be obtained by replacing Equations 17 and 15 with Equation 3 as follows:

$$U_d = \frac{A_d H_d \sigma_c^2}{2[E + \frac{b\sigma_c}{(b-1)}]^2}[E e^{-at} + \frac{1}{K} - \lambda] \tag{18}$$

**Determining the height of destressed zone**

According to Equation 1, the stored strain energy in the mined rock (coal) is equal to the stored strain energy in the caved materials within the destressed zone. Therefore, the substitution of Equations 18 and 2 for Equation 1 leads to the calculation of the height of the destressed zone ($H_d$) in long-term condition as follows:

$$H_d = \frac{\frac{(1+\nu)(1-2\nu)\gamma A_m \sigma_v}{(1-\nu)E}\left[\frac{h_s^2}{3} + H^2 + H h_s\right]}{\frac{A_d \sigma_c^2}{[E + \frac{b\sigma_c}{(b-1)}]^2}[2E e^{-at} + \frac{\sigma_s^{\mu}}{B t^{\alpha}} - \lambda]} \tag{19}$$

All of the incorporated parameters in the aforementioned equation are defined previously.

## RESULTS AND DISCUSSION

### Results verification

To verify the outputs of the current study, obtained results are compared with the results of *in-situ* measurements conducted by other researchers (Haifeng et al., 2011; Zhimin et al., 2010; RafiqulIslam et al., 2009) as well as with the results of analytical model proposed by Rezaei et al. (2015a) in short-term condition. It should be noted that the values of experimental coefficients shown in Table 1 are used in long-term condition calculations. Furthermore, the threshold value of stress ($\sigma_s$) is

**Table 2.** Comparison of the results of suggested model with in-situ measurements.

| No. | Reference | H (m) | $L_w$ (m) | γ ($KN/m^3$) | E (GPa) | ν | $\sigma_c$ (MPa) | b | $h_s$ (m) | $H_d$ (m) | | |
|---|---|---|---|---|---|---|---|---|---|---|---|---|
| | | | | | | | | | | *In-situ* | Short-term condition [4] | Long-term condition (Current paper) |
| 1 | [14] | 285 | 223 | 2.466 | 2.32 | 0.2775 | 31.3 | 1.5 | 4 | 51.7 | 47.72 | 77.81 |
| 2 | [15] | 253 | 200 | 2.6627 | 25.2 | 0.174 | 32.07 | 1.5 | 3.9 | 64.5 | 40.99 | 91.50 |
| 3 | [16] | 290 | 120 | 2.7 | 3.5 | 0.22 | 50 | 1.5 | 3.5 | 29.5 | 23.01 | 31.09 |

Rezaei et al. (2015a).

assumed as the 80% of uniaxial compressive strength of caved materials and the pressure time of caved materials ($t$) is considered 1.5 years. The comparison results are shown in Table 2. As shown in Table 2, the resulted height of destressed zone long-term condition (current study) is in accordance with the results of *in-situ* measurement in dataset 3. Actually, the results of this study and *in-situ* measurements in dataset No. 3 are quite close together. However, the results of the current study are greater than the results of *in-situ* measurements in other two datasets. Also, the long-term condition results are too greater than the results in the short-term condition. This is due to the fact that the full compression of caved materials causes further fracturing and caving of the roof rock strata. Accordingly, the height of destressed zone can be increased during the time. On the contrary, *in-situ* measurements are usually conducted during the mining operations in which the full compression of caved materials is not occurred yet. Also, in short-term condition the effect of pressure time of caved material is ignored causing the height of destressed zone to be decreased compared to the long-term condition. Therefore, it can be concluded that the results of the current study can be consistent with reality in the long-term condition and consequently, these differences are reasonable to some extent.

## Parametric study

Here, actual dataset No. 3 in Table 2 is applied to evaluate the effect of incorporated parameters on the HDZ. In this analysis, constant values of experimental parameters presented in Table 1 were utilized in the parametric study calculations. Similar to the previous sub-section, the threshold value of stress ($\sigma_s$) is considered as the 80% of uniaxial compressive strength of caved materials and the pressure time of caved materials ($t$) is considered 1.5 years in calculations. Accordingly, variation of the height of destressed zone over the longwall gob versus the extracted coal seam thickness is illustrated in Figures 4 and 5, respectively. In these figures, the rest of the parameters are kept constant according to actual data. Also, variations of extracted coal seam thickness and bulking factor are considered between 0 to 5 m and 1.05 to 1.8 (expansion factor 5 to 80%), respectively. Moreover, variations of the height of destressed zone versus the extracted coal seam thickness for different values of depth of cover, panel roof rock's average unit weight, panel roof rock's average elastic modulus, panel roof rock's average Poisson ratio and average uniaxial compressive strength and pressure time of caved materials are as shown in Figures 6 to 11, respectively. In these figures, one of the parameters (chart target parameter) is changed and the rest are kept constant.

As shown in Figures 4 and 5, HDZ has direct and inverse relationships with extracted coal seam thickness and bulking factor, respectively. In Figure 5, the values of 1.05 and 1.8 are considered as the lower and upper limits of bulking factor, respectively. However, it can be concluded from this figure that variations of the height of destressed zone in bulking factors less than 1.1 (expansion factor less than 10%) is relatively high compared to the bulking factors more than 1.1. This result is in agreement with the result reported by Majdi et al. (2012) in which the average expansion factor of 5% and 10% was considered to represent the long-term and short-term conditions of the caved rocks in the goaf area, respectively.

In Figures 6 to 11, the effects of depth of cover, unit weight, elastic modulus, Poisson ration, uniaxial compressive strength pressure time of caved materials on the height of destressed zone are presented. In these figures, relationships between the height of destressed zone and extracted coal seam thickness are potted for different values of the aforementioned variables. For example, the relationships between HDZ and extracted coal seam thickness are as shown in Figure 6 for the different overburden depth. This figure shows that when the depth of cover

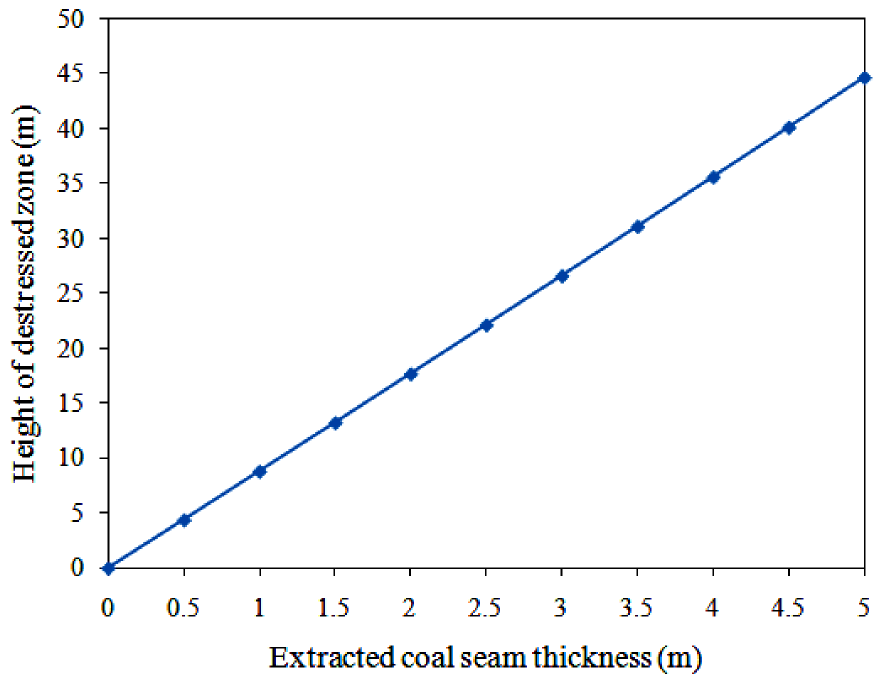


**Figure 4.** Variations of height of destressed zone versus extracted coal seam thickness.

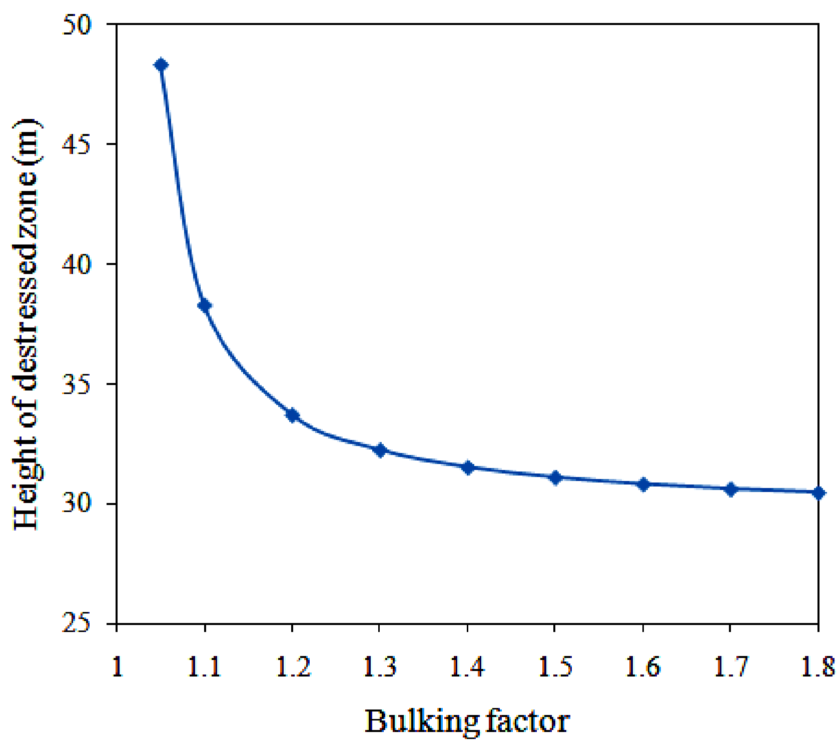


**Figure 5.** Variations of height of destressed zone versus average bulking factor of caved materials.

HDZ would increases,also increase. It can be seen from Figure 7 that HDZ is in direct relation with the panel roof rock's average unit weight. Figure 8 indicates that the higher average elastic modulus of panel roof rocks leads

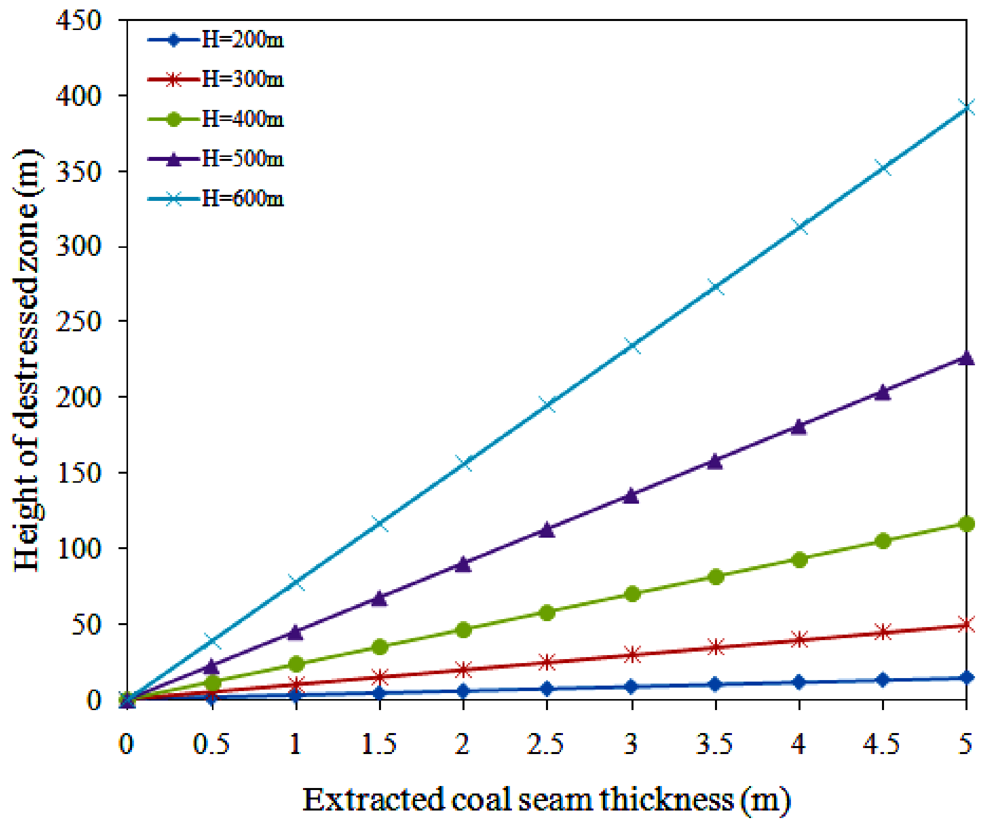


**Figure 6.** Relationship between height of destressed zone and extracted coal seam thickness for different values of depth of cover.

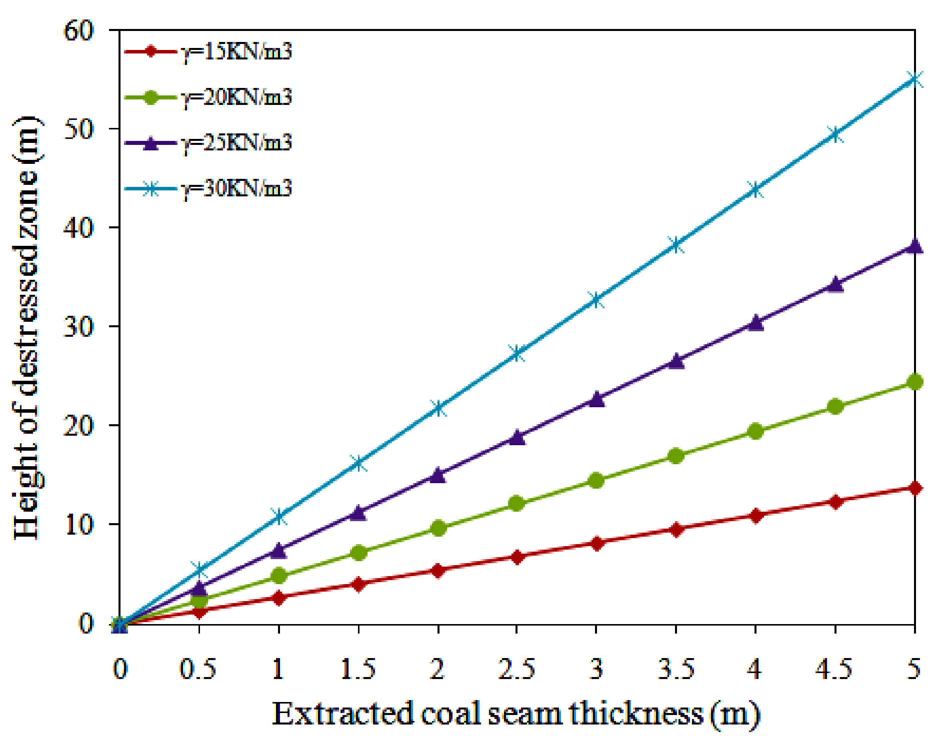


**Figure 7.** Relationship between height of destressed zone and extracted coal seam thickness for different values of panel roof rock's average unit weight.

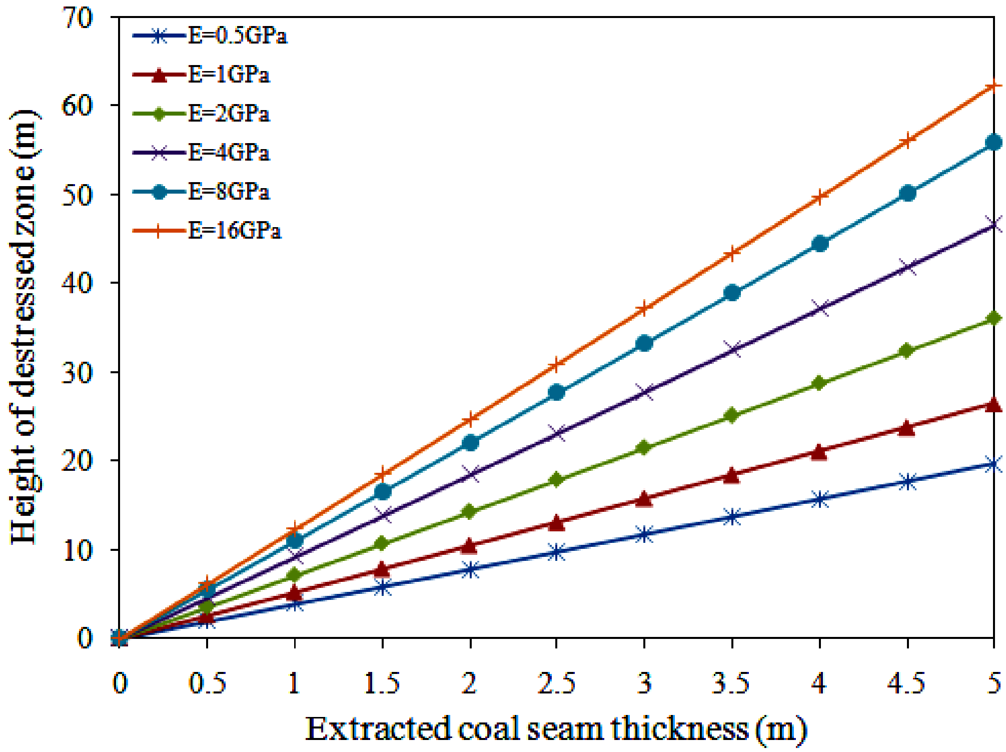


**Figure 8.** Relationship between height of destressed zone and extracted coal seam thickness for different values of panel roof rock's average elastic modulus.

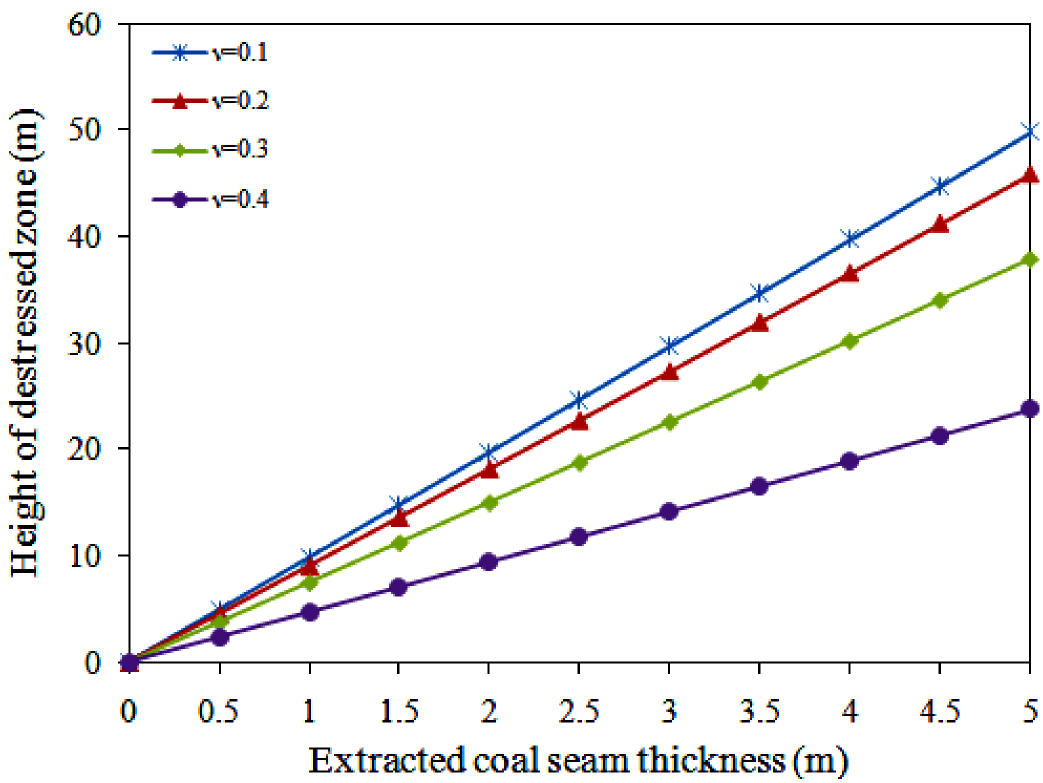


**Figure 9.** Relationship between height of destressed zone and extracted coal seam thickness for different values of panel roof rock's average Poisson ratio.

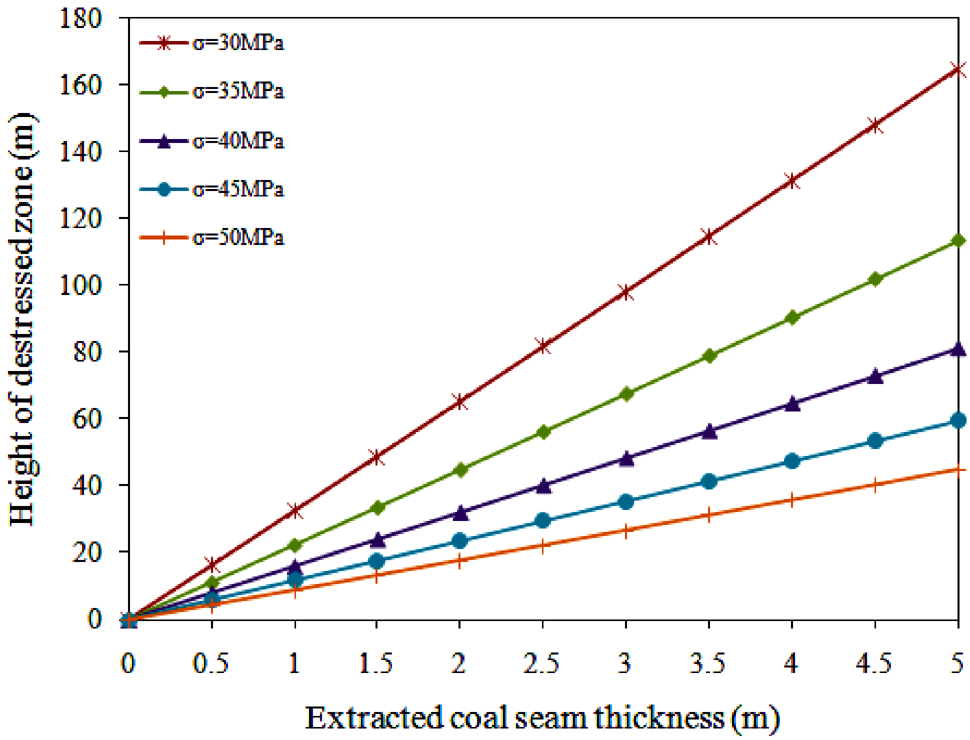


**Figure 10.** Relationship between height of destressed zone and extracted coal seam thickness for different values of average uniaxial compressive strength of caved materials.

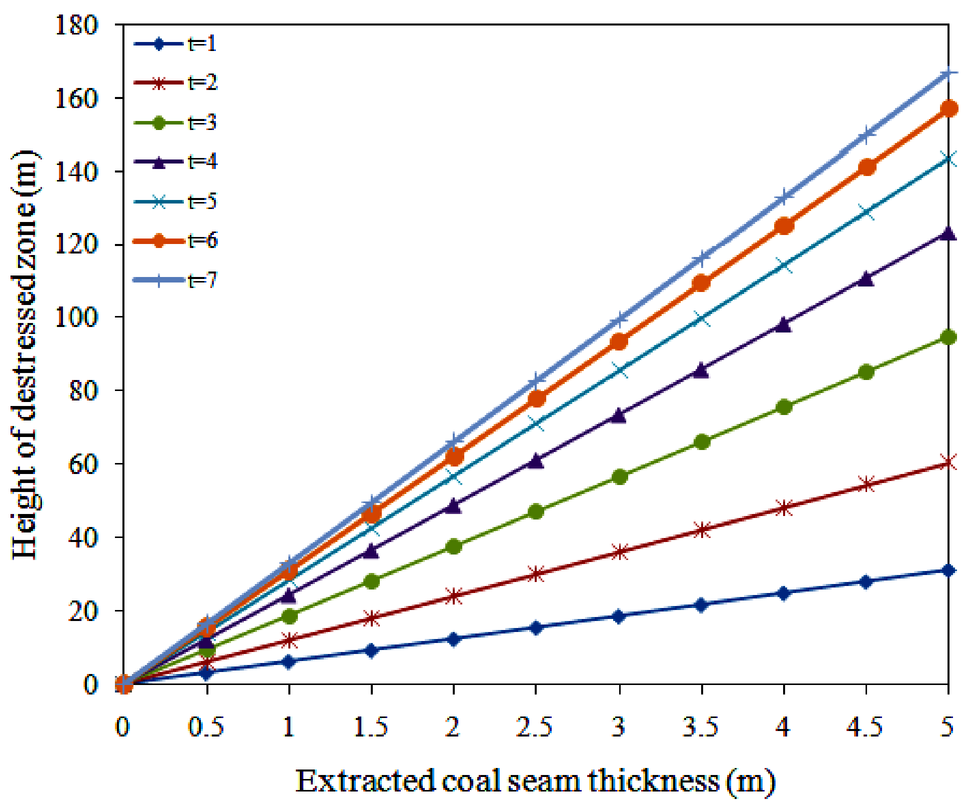


**Figure 11.** Relationship between height of destressed zone and extracted coal seam thickness for different values of pressure time of caved materials.

**Table 3.** Comparison between the results of new model with the results of existing comparable methods (after Rezaei, 2016).

| Method of appraisal | HDZ (×$h_s$) |
|---|---|
| In-situ measurement | 2-100 |
| Empirical model | 2-105 |
| Analytical model | 4.5-48 |
| Numerical model | 5.8-47.6 |
| Short-term model | 2.02-57.8 |
| Artificial neural network model | 2.4-86.5 |
| Multivariate regression analysis model | 10.02-40.93 |
| Long-term model (current study) | 2.7-78.1 |

to the higher HDZ. It can be concluded from Figure 9 that as the panel roof rock's average Poisson ratio increases, the HDZ would decrease. Figure 10 shows that the higher the uniaxial compressive strength of caved materials, the lower the HDZ. Finally, Figure 11 shows that HDZ increases by increasing the pressure time of caved materials.

The ratio between height of destressed zone and extracted coal seam thickness ($H_d/h_s$) resulted from this parametric study can be used as a basis for comparative analysis object with the previous methods in this field. Figure 4 shows as the extracted coal seam thickness varies from 0.5 to 5 m, the ratio of $H_d/h_s$ varies from 8.7 to 8.9. Similarly, it can be concluded from Figures 5 to 11 that the ratio of $H_d/h_s$ varies from 8.7 to 13.8, 2.9 to 78.1, 2.7 to 10.9, 3.9 to 12.4, 4.7 to 9.9, 8.8 to 32.7, and 4.11 to 33.1, respectively. According to the aforementioned analysis, the predicted HDZs in the current study are in the range of 2.7 to 78.1 times the extracted coal seam thickness (Table 3).

## Comparative analysis

In this section, the results obtained from the present study are compared with the comprehensive results of previous methods in this field (Majdi et al., 2012; Rezaei et al., 2015a; Rezaei 2016; Rezaei et al., 2017). Rounding up these literatures, there are numerous empirically and analytically relations as well as numerical, artificial neural network (ANN) and multivariate regression analysis (MVRA) models to estimate HDZ that were found in Rezaei (2016) and Rezaei et al. (2017). Accordingly, the summary results of the previous models in addition to the long-term calculation of HDZ as the coefficient of extracted coal seam thickness ($h_s$) are shown in Table 3. In this table, the results (HDZ) are described based on the coefficient of the extracted coal seam thickness ($h_s$). It can be concluded from this comparison that the lower limit of HDZ calculation in long-term condition is close to the lower limit of other methods especially *in-situ* measurements, empirical model and short-term calculation of HDZ. On the other hand, the upper limit of the HDZ calculation in long-term condition is close to the upper limit of empirical model, ANN model and *in-situ* measurements. Therefore, it can be concluded that the results of the current study are in close agreement with the *in-situ* measurements and other verified models as well. Furthermore, the most important advantage of the current study compared to the other analytical and empirical models is taking into account further effective parameters. In previous empirical and analytical models used to study the roof caving and fracturing behavior, only two parameters including extracted coal seam thickness and average bulking factor are utilized (Peng and Chiang, 1984; Majdi et al., 2012). Also, depth of cover and strength properties were incorporated in short-term prediction of HDZ by Rezaei et al. (2015a) besides two aforementioned parameters. In addition to the aforementioned parameters, the pressure time and temperature-dependent parameters of caved materials are considered in the present study.

Considering the aforementioned results, it is concluded that the results of the current study can be successfully used to study the roof caving and fracturing behavior over the gob in longwall mining. Beyond the calculated HDZ, the overburden weight will be transferred towards the front abutment and the two adjacent neighboring solid sections where the access tunnels, the intervening barrier pillars and the adjacent un-mined solid sections are located. In fact, the difference between the longwall depth ($H$) and the height of destressed zone ($H_d$) must be considered for the calculation of stress transfer towards the adjacent pillars and access tunnels. Another application of roof behavior study in long-term condition is to determine the maximum ground surface subsidence due to longwall mining. It is obvious that the maximum height of destressed zone in longwall mining obtained during the time while the height of destressed zone will be stable. Therefore, further caving is not accrued in the roof strata after the stabilization of the height of destressed zone. If the process of caving and fracturing is stopped and the height of destressed zone is fixed, then stress field of the system will return to its condition before the mining operations. Accordingly, stress transfer to the neighboring solid sections does not occur, nor does additional subsidence takes place in the ground surface.

## Conclusion

In the present research, the roof caving and fracturing behaviors are studied in long-term condition. The conducted theoretical calculations were based on the strain energy balance during the longwall mining along with a constitutive rheological model of caved materials with time-varying parameters. Parametric study was also performed to evaluate the effect of influencing parameters on the HDZ. The results showed that depth of cover, panel roof rock's average unit weight, extracted coal seam thickness, panel roof rock's average elastic modulus and pressure time of caved materials have direct relationships with the HDZ. On the contrary, average uniaxial compressive strength of caved materials, panel roof rock's average Poisson ratio and bulking factor of caved materials have inverse relationships with it. To verify the current study results, calculated HDZ were compared with the results of available previous models as well as with *in-situ* measurements proposed by other researchers. The comparative conclusions have proved that the results of this study are in close agreement with the results of *in-situ* measurements and with the other comparable methods. The general significance of this study is that it incorporates the effects of geometric parameters, roof rock strata properties and pressure time and temperature dependent parameters of caved materials in roof behavior analysis. The long-term evaluation of roof rock strata behavior plays an important role in accurate estimation of transferred loads towards the gates and pillars. In fact, the difference between longwall depth and HDZ must be taken into account in calculation of stress transfer towards the front abutment and the adjacent rib-sides. Furthermore, estimation of this height can help to determine the maximum ground surface subsidence due to longwall mining.

## CONFLICT OF INTERESTS

The authors have not declared any conflict of interests.

### REFERENCES


Gao F, Stead D, Coggan J (2014). Evaluation of coal longwall caving characteristics using an innovative UDEC Trigon approach. Comput. Geotech. 55:448-460.

Haifeng LU, Baoyuan Y, Lin W (2011). Rock parameters inversion for estimating the maximum heights of two failure zones in overburden strata of a coal seam. Min. Sci. Technol. (China) 21:41-47.

Le TD, Mitra R, Oh J, Hebblewhite B (2017). A review of cavability evaluation in longwall top coal caving. International J. Min. Sci.Technol. 27:907-915.

Liu S, Li W, Wang Q (2017). Height of the Water-Flowing Fractured Zone of the Jurassic Coal Seam in Northwestern China. Mine Water Environ. DOI: 10.1007/s10230-017-0501-1.

Majdi A, Hassani FP, Yousef Nasiri M (2012). Prediction of the height of destressed zone above the mined panel roof in longwall coal mining. Int. J. Coal Geol. 62:62-72.

Majdi A, Rezaei M (2013). Application of artificial neural networks for predicting the height of destressed zone above the mined panel in longwall coal mining. 47th US Rock Mechanics/Geomechanics Symposium, San Francisco, California, USA, 1665-1673.

Palchik V (2003). Formation of fractured zones in overburden due to longwall mining. J. Environ. Geol. 44(1):28-38.

Peng S, Chiang H (1984). Longwall Mining. New York: Wiley.

RafiqulIslam MD, Hayashi D, Kamruzzaman ABM (2009). Finite element modeling of stress distributions and problems for multi-slice longwall mining in Bangladesh, with special reference to the Barapukuria coal mine. Int. J. Coal Geol. 78(2):91-109.

Rezaei M (2016). Development of an intelligent model to estimate the height of caving-fracturing zone over the longwall gobs. Neural Comput & Applic. DOI: 10.1007/s00521-016-2809-3.

Rezaei M, 2017. Long-term stability analysis of goaf area in longwall mining using minimum potential energy theory. J. Min. Environ. Doi: 10.22044/jme.2017.5950.1408.

Rezaei M, Hossaini MF, Majdi A (2015a). A time-independent energy model to determine the height of destressed zone above the mined panel in longwall coal mining. Tunnel. Undergr. Space Technol. 47:81-92.

Rezaei M, Hossaini MF, Majdi A (2015b). Development of a time-dependent energy model to calculate the mining-induced stress over gates and pillars. J. Rock Mech. Geotech. Eng. 7(3):306-317.

Rezaei M, Hossaini MF, Majdi A, Najmoddini I (2017). Determination of the height of destressed zone above the mined panel: An ANN model. Int. J. Min. Geo-Eng. 51(1):1-7.

Salamon MDG (1990). Mechanism of caving in longwall mining. Rock Mechanics Contributions and Challenges: Proceedings of the 31st US Symposium, Golden. pp. 161-8.

Shen L, Chaojun F, Mingkun L, Zhenhua Y, Tianwei L, Haifeng Z (2017). Structure and deformation measurements of shallow overburden during top coal caving longwall mining. Intl. J. Min. Sci. Technol. 27:1081-1085.

Wang S, Li X, Wang S (2017). Separation and fracturing in overlying strata disturbed by longwall mining in a mineral deposit seam. Eng. Geol. 226:257-266.

Yavuz H (2004). An estimation method for cover pressure re-establishment distance and pressure distribution in the goaf of longwall coal mines. Int. J. Rock Mech. Min. Sci. 4:193-205.

Zhang T, Ma M, Wang H, Xu H (2011). A nonlinear rheological model of backfill material for retaining roadways and the analysis of its stability. Min. Sci. Technol. (China) 21:543-546.

Zhimin X, Yajun S, Qinghong D, Guowei Z Shi L (2010). Predicting the height of water-flow fractured zone during coal mining under the Xiaolangdi Reservoir. Min. Sci. Technol. 20:434-438.